Ecological Processes

RESEARCH Open Access

# The spatial variability of actual evapotranspiration across the Amazon River Basin based on remote sensing products validated with flux towers

Victor Hugo da Motta Paca[1,2,3*], Gonzalo E. Espinoza-Dávalos[1], Tim M. Hessels[1,2], Daniel Medeiros Moreira[3], Georges F. Comair[4] and Wim G. M. Bastiaanssen[1,2]

## Abstract

Actual evapotranspiration (ET) is a major component of the water balance. While several international flux measurement programs have been executed in the tropical rain forest of the Amazon, those measurements represent the evaporative process at a few selected sites only. The aim of this study is to obtain the spatial distribution of ET, using remote sensing techniques, across the entire Amazon River Basin. Results from six global ET products based on remote sensing techniques (GLEAM, SEBS, ALEXI, CMRSET, MOD16, and SSEBop) were merged to obtain an ensemble prediction of the ET rates for the complex and in-accessible environment of the Amazon at a spatial resolution of 250 m. The study shows that the basin-wide average ET is 1316 mm/year with a standard deviation of 192 mm/year. This new ET-Amazon product was validated against seven different historic flux tower measurements. The energy balance closure of the in situ measurements varied between 86 and 116%. Only months with more than 70% completeness of in situ measurements were considered for validation. Different procedures for closure correction were included in the analyses. The correlation between measured and remotely sensed ET is good ($R^2 > 0.97$ for consecutive periods of 2 to 12 months), and the bias correction is negligible for the energy balance residual method, which seemed most favorable. Monthly ET values have more uncertainty. The monthly RMSE values vary between 7.4 and 27.8 mm/month (the average RMSE is 22.2 mm/month), and the coefficient of determination ($R^2$) varies between 0.48 and 0.87 (the average $R^2$ is 0.53). The ET from the water balance is 1380 mm/year, being − 64 mm/year difference and 4.6% less than ET derived from the water balance. The evaporation from the Amazon basin inside Brazil is 5063 km$^3$/year, followed by Peru with 1165 km$^3$/year. ET-Amazon shows more spatial details and accuracy than alternative global ET products such as LandFlux-EVAL, Model Tree Ensemble (MTE), and WACMOS-ET. This justifies the development of new regional ET products.

**Keywords:** Amazon River Basin, Evapotranspiration, Flux towers measurements, ET-Amazon product

## Introduction

The hydro-climatic regime of the Amazon River Basin has a fundamental influence on the climate of South America and the globe (Fisch et al. 1998; Malhi et al. 2015; Nobre et al. 2016). The hydrology of the Amazon is dependent on the water, heat, and carbon exchanges between land and atmosphere. These processes in the Amazon rain forest are important for global carbon sequestration and biodiversity and play a critical role in regulation of the regional and global climate. Given the large amount of carbon stored in the Amazon forests, there is considerable potential to influence the global climate if not properly protected or managed. Due to continental-scale atmospheric moisture recycling processes (e.g., Mohamed et al. 2005; van der Ent et al. 2012), rainfall in the Southern Region of Brazil and South America depends on the evapotranspiration of the Amazon (Salati et al. 1979; Nobre 2014). Yet, due to its immense dimensions and

* Correspondence: victorpaca@yahoo.com
[1]IHE Delft Institute for Water Education, Westvest 7, Delft 2611 AX, Netherlands
[2]TU Delft, Delft, Netherlands
Full list of author information is available at the end of the article

natural land cover, this ecosystem is only partially understood.

In recent years, the hydrology was characterized by large fluctuations in wet and dry years (Costa and Foley 1999; Marengo 2006; Davidson et al. 2012; Gloor et al. 2013; Lopes et al. 2016). Major floods occurred during 2009, 2012, 2014, and 2015 (Marengo and Espinoza 2016). In contrast, 2005 and 2010 were characterized by severe droughts (Nobre 2013). These increasing fluctuations of rainfall and streamflow raise severe environmental and agricultural concerns, and local authorities need to improve their assessment of droughts and floods and the impact thereof on livelihood and ecosystems. A reanalysis of these extreme events that occur in such a short period of time cannot be undertaken without having a deeper understanding of the bio-physical processes, and local evapotranspiration (ET) in particular. Hydrologically based water accounting should be applied for systematic reporting on the water resources of the Amazon basin (e.g., Bastiaanssen and Chandrapala 2003; Karimi et al. 2013).

The hydrological observation network in the Amazon forest is neither meeting the required density nor delivers complete time series adequate for making operational assessments of river flow (Paca et al. 2011). Incomplete observations hamper the process of obtaining reliable streamflow and flood predictions. The conversion of precipitation into streamflow is classically done by means of rainfall–runoff models (e.g., Duan et al. 1992). More recently, results were published where runoff is determined from remotely sensed rainfall and ET values in ungauged basins (e.g., Simons et al. 2016; Poortinga et al. 2017). Predictions of ET in conjunction with satellite estimates of precipitation and water storage provide a new methodology to predict streamflow in river basin (e.g., Liu et al. 2016). Such predictions can be improved if accurate ET maps of the Amazon are available.

The number of ET studies in the Amazon basin, based on water budget analysis and climatological and aerological methods by Marques (1980) and Salati (1987), has increased since the beginning of the 1970s. The average actual ET values in the entire Amazon basin were estimated to vary between 1000 and 1905 mm/year. Using isotopes, Marques (1980) obtained ET values between 1146 and 1260 mm/year, being much lower than those found by Salati (1987).

The first ET studies based on flux tower measurements in the Amazon basin were done during the Amazonian Research Meteorological Experiment (ARME) in 1983 at the city of Manaus (Fisch et al. 2008). The next expeditions are referred to as the Atmospheric Boundary Layer Experiments (ABLE2A and ABLE2B) in 1989 (Harris 2008). Shuttleworth (1988) calculated ET at the Ducke forest reserve 25 km from Manaus, and the near K34 site, and reported values ranging between 1288 and 1344 mm/year over 2 years of combined in situ measurements and calibrated modeling. His values were lower than those of Salati (1044 to 1560 mm/year), but higher than those of Marques (1146 to 1260 mm/year). These were the first in situ measurements based on eddy covariance techniques, which provided the basis for a follow-up project: the Anglo-Brazilian Amazonian Climate Observation Study (ABRACOS). The study included six flux towers in forest and grassland, in the cities of Manaus, Marabá, and Ji-Paraná from 1991 until 1995. The ET measured during the experiment ranged from 2.1 to 3.8 mm/day or from 768 to 1392 mm/year (Gash et al. 1996).

The ET studies in the Amazon basin culminated into the Large-Scale Biosphere-Atmosphere Experiment in the Amazon (LBA) (Saleska et al. 2013; de Gonçalves et al. 2013). The LBA flux database is one of 12 from the Earth Observing System Data and Information System (EOSDIS). Da Rocha (2009) reviewed the ET measurements and estimates from LBA and recorded a range of 2.7 to 6 mm/day (i.e., 986 to 2190 mm/year, assuming these measurement days are representative of the year). Hence, after more than 40 years of research, ET statistics (mean, standard deviation, range) for the basin as a total ecosystem are still under discussion and review.

Von Randow et al. (2004) analyzed the energy balance closure with data from the Rondônia stations and concluded that the energy balance did not close due to (1) slow wind speed, (2) short timescales causing failure of instruments to record eddy processes, and (3) significant amounts of energy being transported horizontally. A bias correction on the energy balance parameters was proposed similar to the corrections on the eddy correlation fluxes of croplands in the semi-arid regions of Brazil (Teixeira and Bastiaanssen 2012).

Due to a low density of stations and scaling point data relative to the areas involved, the flux tower data cannot be a true reflection of the average ET over the whole basin. This was pointed out in earlier large-scale energy and water balance field experiments such as EFEDA (Pelgrum and Bastiaanssen 1996), FLUXNET sites (Wilson 2002), and fluxes measured in ecosystems (Nagler et al. 2005). While flux towers provide local ET estimates, the spatial variability of ET across the Amazon is poorly understood. Hence, methodologies need to be developed that describes the full variability of ET fluxes, and remote sensing technique is one of them.

The spatial variability and magnitude of ET can be described by means of remote sensing technologies with an acceptable accuracy, especially when the fluxes are integrated across a longer period (e.g., Kustas et al. 2003; Jia et al. 2010; Karimi and Bastiaanssen 2015). This study includes global scale state-of-the-art procedures to estimate ET for the complete Amazon basin for a period of 10 years (2003 to 2013) (Appendix 1 and Appendix 2). The availability of global ET data sets from individual (GLEAM, SEBS, ALEXI, CMRSET, MOD16, SSEBop) remote sensing products will create new opportunities to determine local ET fluxes, also when no in situ instruments are available. The objective of this study is to develop a high resolution spatially distributed ET map (250 m × 250 m) for the entire Amazon basin—thus also from upstream countries—based on existing remote sensing models and validated against independent flux towers installed over different land use classes.

## Material and methods

### Climatology

The Amazon River Basin covers $6.1 \times 10^6$ km$^2$ and extends over seven countries. The percentages of each country covered by the basin are as follows: Brazil (63%), Peru (16%), Bolivia (12%), Colombia (5.6%), Ecuador (2.3%), Venezuela (0.8%), and Guyana (0.3%) (Villar 2009) (Fig. 1). The annual mean precipitation in the Amazon basin based on rain gauges is 2460 mm/year (CPRM 2011). Areas with high rainfall occur on the slope of the Andes Mountains (6000 mm/year) and near the coast at the north-east region in Amapá (4000 mm/year). The minimum rainfall is 600 mm/year, and it occurs at the central Brazilian plateau (Fisch et al. 1998, Braga et al. 1999, and CPRM 2011). Figure 1 shows the boundaries, the hydrographic network obtained from the ORE-HYBAM database (http://www.ore-hybam.org), the location of two climatological stations of which data were obtained from SISDAGRO/INMET (http://sisdagro.inmet.gov.br/sisdagro/app/index), and the seven flux tower locations from LBA project (https://daac.ornl.gov).

The monthly distribution of rainfall and standard reference evapotranspiration ($ET_0$) for two selected upstream and downstream meteorological stations in the Amazon are depicted in Fig. 2. The data are from the stations of Rio Branco, in the State of Acre, and Porto de Moz, in the State of Pará, both in Brazil. The Rio Branco station is in the capital of the State of Acre, in Brazil, near the Acre River, which is part of the Purus River Basin. The Porto de Moz station is in the Low Amazon Mesoregion, in the mouth of Xingu River; both stations are at the right side of the river bank of the Amazon River.

The rate of actual ET is mainly driven by climatic variables, soil moisture, and leaf area index. Reference evapotranspiration ($ET_0$) integrates climatic data such as cloud cover, solar radiation, temperature, air humidity, and wind speed into one single parameter, which is plotted against rainfall for the two climatological stations in Fig. 2. The $ET_0$ was obtained from the FAO-56 standard Penman-Monteith equation. The plot of rainfall and $ET_0$ gives an indication of the monthly climatic conditions of the region. At the Porto de Moz station, average precipitation over the period 2011 to 2013 was 205 mm/month and $ET_0$ 72 mm/month. The precipitation at Rio Branco was on average 177 mm/month and $ET_0$ is 68.3 mm/month. The monthly variability in the downstream part

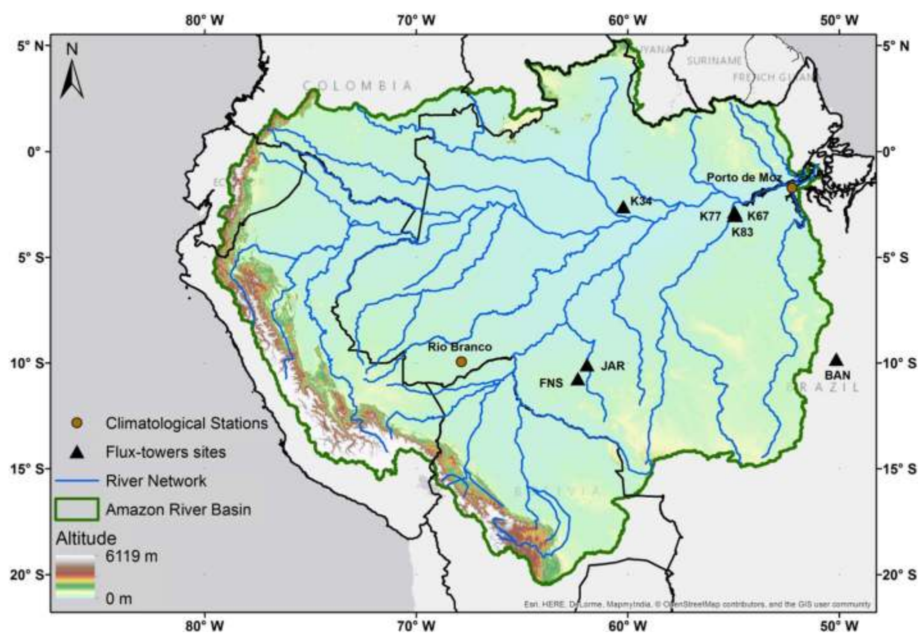


**Fig. 1** Location of the Amazon River Basin. The altitude is taken from the USGS Digital Elevation Model (USGS, 2004). The location of the flux tower sites (black triangles) and two meteorological stations (brown dots) are indicated

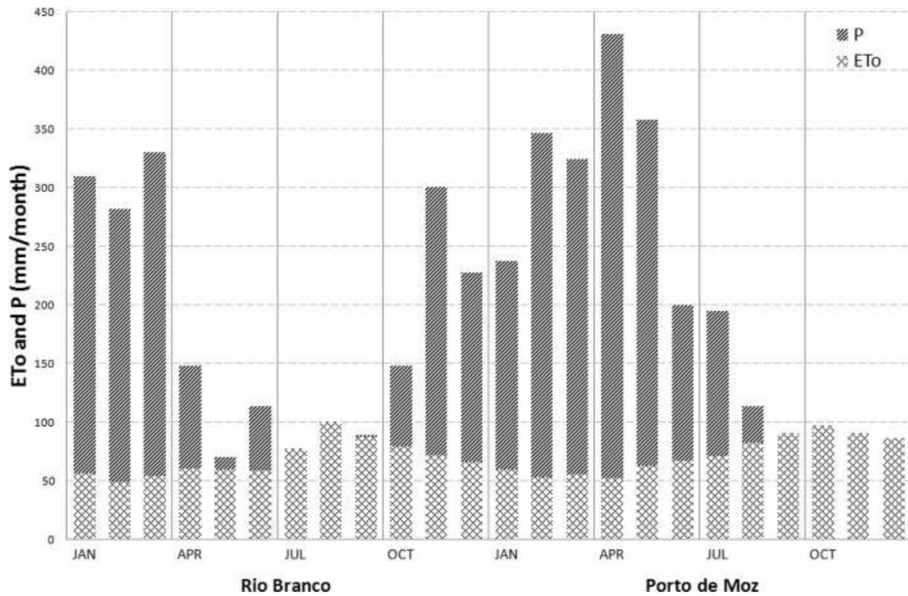


**Fig. 2** Mean monthly precipitation (*P*) and reference evapotranspiration ($ET_0$) values for the period 2011 to 2013 at the Rio Branco (left) and Porto de Moz (right) stations (source INMET, 2017). Two major seasons are observed: (1) the rainy season starting from December until May and (2) the dry season from June to November. These patterns are more pronounced at the Porto de Moz station near the East Coast. Rio Branco reveals water shortage during July ($ET_0 = 78.3$; $P = 38.2$ mm/month) and August ($ET_0 = 100.2$; $P = 58.6$ mm/month). The dry period in Porto de Moz is also longer, suggesting an east-west gradient from the coast to the upper parts of the Amazon basin. Over the 3 years (2011 to 2013), there was a water-deficit at Porto de Moz, in September ($ET_0 = 90.4$; $P = 62.1$ mm/month), October ($ET_0 = 97.2$; $P = 63.8$ mm/month), and November ($ET_0 = 90.3$; $P = 42.9$ mm/month)

of the basin (i.e., Porto de Moz) shows more climatic variability.

### LBA flux tower database

LBA fluxes over the period 2003 to 2013 were used for the ground truth comparison (Saleska et al. 2013). The data is only partially accessible through the website https://daac.ornl.gov for the 1999 to 2006 period and for four stations. The remaining three datasets were acquired from contacting the principal investigators. The description of the flux tower sites and duration of ET data records are presented in Table 1.

The Manaus site (K34) is a primary forest area 60 km from Manaus. This flux tower has the longest recorded data series covering a period of 23 months. Of the months available, 14 was used for this study, since 9 months were before January 2003.

Three flux tower stations are located in Pará State (Santarém) of which station K77 and station K83 were de-activated, and K67 continues collecting data up to

**Table 1** Flux tower sites in the Amazon River Basin and period of available data for the present study

| Tower code | Location | Vegetation type | Lat, Lon | Tower height (m) | Period of available data for this study | Effective months available |
|---|---|---|---|---|---|---|
| K34 | Amazonas, Manaus | Primary forest | − 2.609, − 60.209 | 53 | 1999/2006 | 23 |
| K67 | Pará, Santarém | Primary forest | − 2.857, − 54.959 | 63 | 2008/2011 | 25 |
| K77 | Pará, Santarém | Agriculture field | − 3.02, − 54.894 | 18 | 2001/2004 | 5 |
| K83 | Pará, Santarém | Primary forest | − 3.018, − 54.971 | 64 | 2001/2003 | 12 |
| BAN | Tocantins, Ilha do Bananal | Cerrado and pasture | − 9.824, − 50.159 | 40 | 2003/2006 | 18 |
| FNS | Rondônia, Ouro Preto do Oeste | Pasture | − 10.750, − 62.367 | 8 | 2009/2010 | 10 |
| JAR | Rondônia, Ji-Paraná | Primary forest | − 10.083, − 61.931 | 63 | 2004/2009 | 27 |

date. Data collected from K67 during 2008 to 2011 were used for the current remote sensing study. These three flux towers were all within a radius of 18 km, as shown in Fig. 1 and described in Table 1.

The BAN flux tower is located in Tocantins State and has been dismantled, but enough data for the period 2003 to 2006 were available for our purpose.

The flux towers Rebio-Jaru (JAR) and Fazenda Nossa Senhora (FNS) are located in the State of Rondônia, but only the latent heat flux was included in this study. Both stations are still working.

More information on the sites are given in Fig. 1, Table 1, and Appendix 4.

The distance between the seven stations is large, and consequently, their ecosystems, physical land surface conditions, and climatology differ vastly, which contributes to getting a regional picture of ET fluxes. All flux towers are based on the eddy covariance method. The turbulent fluxes and the vertical profiles of $CO_2$ concentration, air humidity, and air temperature are measured above the canopy at heights ranging between 8 and 64 m above ground level. Staff security and extreme weather conditions are practical limitations to collect complete datasets. The long exposure to thunderstorms and disappearance of solar panels and batteries have led unavoidably to periods of missing data. The incomplete time series is a limitation for validating monthly ET products from remote sensing technologies. Only months with 70% complete data sets—or longer—were included for the validation in the current study. The JAR flux site, with 27 months of data, provided the most complete time series.

### Interpretation of surface energy balance measurements

The land surface fluxes are coupled by means of the surface energy balance equation:

$$\lambda E = R_n - H - G \tag{1}$$

where $\lambda E$ is the latent heat flux density associated with actual evapotranspiration, $R_n$ is the net radiation flux density, $H$ is the sensible heat flux density, and $G$ is the soil heat flux density. Values of $\lambda E$ flux densities (W/m$^2$) were converted into ET rates (depth per unit time) using Eq. (2):

$$\mathrm{ET} = \frac{\lambda E}{\lambda\, \rho w} \tag{2}$$

where $\lambda$ (MJ/kg) is the latent heat of vaporization (2.45 MJ/kg at 25 °C) and $\rho_{\mathrm{w}}$ (kg/m$^3$) is the density of water. Three different data interpretation methods were used to obtain monthly ET data from LBA flux towers: (1) direct measurement of latent heat flux $\lambda E$, (2) residual of the energy balance closure method ($\lambda E = R_n - G - H$), and (3) the Bowen ratio closure forcing method (see Eq. 3). The first method directly measures the $\lambda E$ fluxes using the eddy flux equipment. Araújo et al. (2002) and Restrepo-Coupe et al. (2013) used this method for LBA ET rates. According to von Randow et al. (2004), the direct $\lambda E$ fluxes are underestimating ET for pasture land, and forests, so direct flux measurements must be interpreted with caution. The energy balance closure method was evaluated by von Randow et al. (2004) for two sites in the south-western Amazon (FNS and JAR flux towers). The residual method was applied if $\lambda E$ measurements were less accurate than measurements of $H$. The Bowen ratio method (3) uses the sensible heat flux $H_{\mathrm{raw}}$ to latent heat flux $\lambda E_{\mathrm{raw}}$ ratio (e.g., Twine et al. 2000) to force the energy balance to close for cases where $H$ and $\lambda E$ have the same degree of error:

$$\lambda E = \frac{R_n - G}{1 + \left(\frac{H_{\mathrm{raw}}}{\lambda E_{\mathrm{raw}}}\right)} \tag{3}$$

The Bowen ratio method described in Eq. (3) is quite popular, but it does not always provide the best results. It is beyond the scope of the current paper to discuss all measurement principles and interpretation methods at length. Instead, a pragmatic approach was undertaken to interpret the results for the three different closure methods and to pinpoint the uncertainty related to eddy covariance measurements in general. By absence of net radiation or soil heat flux data, the FNS and JAR flux towers were considered as direct $\lambda E$ measurements only.

The validation considered different footprints of the flux towers. The footprint analysis ranged from one single pixel (250 m × 250 m) to 7 × 7 pixels (1750 m × 1750 m) assuming the flux towers to be present in the center of the areas of interest. A rule of thumb is that the required fetch should be 10 times the height of the flux measurements. In our case, this would be a minimum fetch requirement of 80 to 640 m. Considering that the routine pixel size of most ET products is 1000 m, a downscaling to 250 m is required. For a single 250 m pixel, the upwind distance will be half, hence 125 m. For seven pixels, the upwind distance is 875 m. Hence, the particular pixels selected represent the water vapor source areas of the fluxes measured by the towers.

The LBA flux database has missing data. The data series were classified into three categories (i.e., 100%, 85%, and 70% completeness). The gaps were filled with the mean daily values for a given month for the 85% and 70% categories. Periods with less than 70% of complete data series were excluded from further analyses.

### Flux measurements

K34 provided 23 months of data records, of which 7 months were 100% complete, 8 months with 85% (i.e., 15% missing records), and another 8 months with 70% data available (i.e., 30% missing records). The monthly

ET rates in the primary forest ranged from 72 mm/month in April 2006 to double the amount (141 mm/month) in October 1999. The Porto de Moz station shows the highest $ET_0$ rates also to occur during October and November; hence, the actual ET fluxes seem to follow the climate demand.

K67 is located in a primary humid tropical forest type. There were 25 months available for the analysis; 19 months contained complete data records and 6 months had 85% complete data. The monthly ET rates varied between 64 mm/month (September 2009) and 132 mm/month (October 2010).

Flux tower K77 is located in an agriculture field and had 9 months of 100% complete data series. Three months had 85% completeness. Five months were available after 2003 for comparison with the ET-Amazon. The ET rates varied between 66 (November) and 151 mm/month (April). K83 in the eastern Amazon had 5 months of useable ET data records only, with 70% complete daily total flux data sets. The ET values measured varied between 126 and 159 mm/month. BAN is located in the Tocantins River Basin, just outside the boundaries of the Amazon River Basin. Because of the inclusion of a vegetation transition zone with pastures and savanna, this station was an attractive option to add for validation of the ET-Amazon product. BAN had 1 month with 100% complete data sets, 6 months with 85%, and 11 months with 70% data sets. The FNS and JAR sites provided direct $\lambda E$ measurements from both flux towers. The FNS showed the lowest ET, 85 mm/month recorded in February 2009, and the highest value of 135 mm/month in March 2010.

The overall situation on the energy balance closure is presented in Table 2. The differences between the three energy balance closure methods did not exceed 25 mm/month, and the maximum difference occurred at site K77. An error of 25 mm at an average monthly ET rate of 125 mm would imply an error of 20%, which agrees with findings in the international literature on eddy covariance measurements. Site K67 had the smallest variability among the three interpretation methods utilized. The surface energy balance closure was 97%.

The overall conclusion of this quality control check is that ET measurements in the Amazon have considerable uncertainties. The lowest energy balance closure was 86% (K34) and the highest 116% (K77). At shorter time scales, the field measurements become even more uncertain. This poses a limitation to the validation of ET Amazon, but remains to be in line with the quality of flux data acquired in other flux sites.

### ET-Amazon product

The spatial variability of ET in the Amazon basin was determined by using the data layers from six existing global scale ET products. They are based on physics and have a global coverage, making them attractive for various types of applications. All ET products used are based on multi-spectral satellite measurements and surface energy balance models: (1) MODIS Global Terrestrial Evapotranspiration Algorithm (MOD16) (Mu et al. 2011), (2) Atmosphere-Land Exchange Inverse Model (MOD16) (Anderson et al. 2007), (3) Global Land Evaporation Amsterdam Model (GLEAM) (Miralles et al. 2011), (4) Surface Energy Balance System (SEBS) (Su 2002), (5) Operational Simplified Surface Energy Balance (SSEBop) (Senay et al. 2013), and (6) CSIRO MODIS Reflectance-based Evapotranspiration (CMRSET) (Guerschman et al. 2009). The main characteristics of each ET product are described in Table 3. Appendix 3 specifies the source of each product.

The underlying models have different parameterizations and use different input data, so their ET predictions cannot be the same (but similar). The usage of different ET products will inherently create a range of ET values for every pixel. This approach is preferred above the usage of one single model. While one ET model will perform better on a certain location, a different ET model will perform better on a different location. Michel et al. (2016) in their WACMOS-ET study tested several individual remote sensing ET layers and concluded that there is no single best performing model across all biome types in the USA and Europe. The same was concluded by Ramoelo et al. (2014) in South Africa. An ensemble ET value is acceptable under data sparse circumstances. The objective of the paper is to get better estimates of ET variability across the Amazon and not a comparison of

**Table 2** Energy balance closure statistics at the LBA flux sites and ET measurement results showing uncertainty compared to ground truth data. The standard deviation is indicated between brackets

| Tower code | Average energy balance closure, $R_n - G - H - \lambda E$ (W/m$^2$) | Average energy balance closure, $\{(H + \lambda E)/(R_n - G)\} \times 100\%$ (%) | Direct method (mm/month) | Residual method (mm/month) | Bowen ratio method (mm/month) | ET difference between methods (mm/month) |
|---|---|---|---|---|---|---|
| K34 | 17.9 | 86 | 102.9 (17.5) | 124.0 (18.9) | 120.2 (19.1) | 21.1 |
| K67 | 2.3 | 97 | 99.7 (18.8) | 108.5 (40.5) | 110.4 (63.4) | 10.7 |
| K77 | − 18.5 | 116 | 106.4 (26.5) | 80.9 (27.4) | 88.7 (22.6) | 25.5 |
| K83 | 5.6 | 95 | 133.9 (6.8) | 146.9 (8.9) | 144.1 (7.3) | 13.0 |
| BAN | 12.8 | 90 | 111.6 (18.9) | 128.1 (11.1) | 123.6 (11.6) | 16.5 |

**Table 3** Description of the ET products selected for ET-Amazon

| Product | Spatial Resolution | Temporal Resolution | Version | Latitudes | Ongoing product until present | Main Data Input |
|---|---|---|---|---|---|---|
| GLEAM | 0.25° | Daily | V2b | 50° N–50° S | Yes | PMW |
| SEBS | 0.05° | Monthly | V0 | 40° N–40° S | Yes | VNIR, TIR |
| ALEXI | 0.05° | Daily | – | 70° N–60° S | Yes | VNIR, TIR |
| CMRSET | 0.05° | Monthly | V1405 | 90° N–90° S | No | VNIR, SWIR |
| MOD16 | 0.01° | 16 days | MOD16A2 | 90° N–90° S | No | VNIR |
| SSEBop | 0.01° | Monthly | – | 90° N–90° S | Yes | TIR |

*VNIR* visible near infrared, *SWIR* shortwave infrared, TIR thermal infrared, PMW is passive MicroWave

models in a data-poor environment. ET-Amazon is therefore based on a linear averaging of the six individual ET products, and subsequently downscaling to 0.0025° using the MODIS-based, normalized difference vegetation index (NDVI) data (Rouse et al. 1973). A priori information on certain ET product performances in the humid forests of Amazon was not convincing, as most ET products have been validated over natural ecosystems. An earlier study using the same six ET products in the Nile basin concluded that an ET product based on simple linear averaging was more congruent with the water balance of river sub-basins than individual ET products (Hofste 2014). A similar conclusion was drawn by Prior (2016) for the Niger basin where the average value of six different ET products was in best agreement with river flow measurements. We adopted the same pragmatic linear averaging approach in order to minimize negative bias from individual ET models. The same argument applies also to ensemble predictions of weather and stream flow forecasts.

The ET predictions of all six models were compared for each pixel, and outlier predictions of individual ET products were rejected. The coefficient of variation between the six ET estimates was used as the metric for rejection. Each pixel in ET-Amazon represents the mean of minimally two or maximally six ET products, although in the majority of cases, it will be based on five to six products.

ET-Amazon was generated in monthly time steps from January 2003 to December 2013 with a pixel size of 0.0025° × 0.0025° (approximately 250 m) following the methodology outlined in Fig. 3. The ET products were resampled (nearest neighbor) to match the pixel size of all the different ET products without modifying the original values. Downscaling to a 0.01° spatial resolution was needed for GLEAM, SEBS, ALEXI, and CMRSET. Downscaling of the ET products was created with the fraction of Absorbed Photosynthetical Radiation (fPAR), being a function of NDVI. It is widely accepted that fPAR behaves linearly with biomass production and Net Primary Production (NPP) and that biomass and transpiration fluxes behave linearly as well (Steduto 2007). The within variability of fPAR in a larger fPAR pixel <fPAR> can be used as a surrogate of ET/<ET>. The chevron brackets describe the areal mean value of the larger pixel. This method ensures that the total ET of the large pixel <ET> remains conserved, but is broken down into smaller pieces:

$$\mathrm{ET} = \mathrm{fPAR}/\langle \mathrm{fPAR} \rangle \times \langle \mathrm{ET} \rangle \quad (4)$$

MODIS-based NDVI data has been used to assess the spatial fPAR grids using the relationship provided by Bastiaanssen and Ali (2003):

$$\mathrm{fPAR} = -0.161 + 1.257\ \mathrm{NDVI} \quad (5)$$

For each pixel, the coefficient of variation (CV) between the different ET products is computed. When CV exceeds 0.5, the one ET product causing the variability will be rejected, and the CV is recomputed. The CV threshold for rejecting outliers is inversely proportional to the ET values when ET is smaller than 10 mm/month. A small difference between ET products at low absolute ET values increases CV, and this effect should be regulated. The criteria for rejection are specified as follows:

$$\mathrm{Outlier} = \begin{cases} \mathrm{ET} < 10\ \mathrm{mm/month} : \mathrm{CV} > 0.5 + 0.15(10\text{–}\mathrm{ET}) \\ \mathrm{ET} > 10\ \mathrm{mm/month} : \mathrm{CV} > 0.5 \end{cases} \quad (6)$$

After removing the outliers, the linear average ET product is downscaled by NDVI towards a resolution of 0.0025°. The ET-Amazon product excludes water pixels. The diagram of the ET-Amazon algorithm is visualized in Fig. 3.

### The water balance closure at regional scale

Local validation of fluxes is a necessity, but it does provide insights on the model performance for thousands of pixels. Validation of remote sensing ET values at a large scale is done classically by means of water balances (e.g., Bastiaanssen et al. 2002; Wu et al. 2012):

$$\Delta S(t) = \int [P(t) - \mathrm{ET}(t) - Q(t)]dt \quad (7)$$

where $\Delta S(t)$ is the water storage change, $P(t)$ is the precipitation, $\mathrm{ET}(t)$ is the actual evapotranspiration (mm/year), and $Q(t)$ is the runoff leaving the domain to which

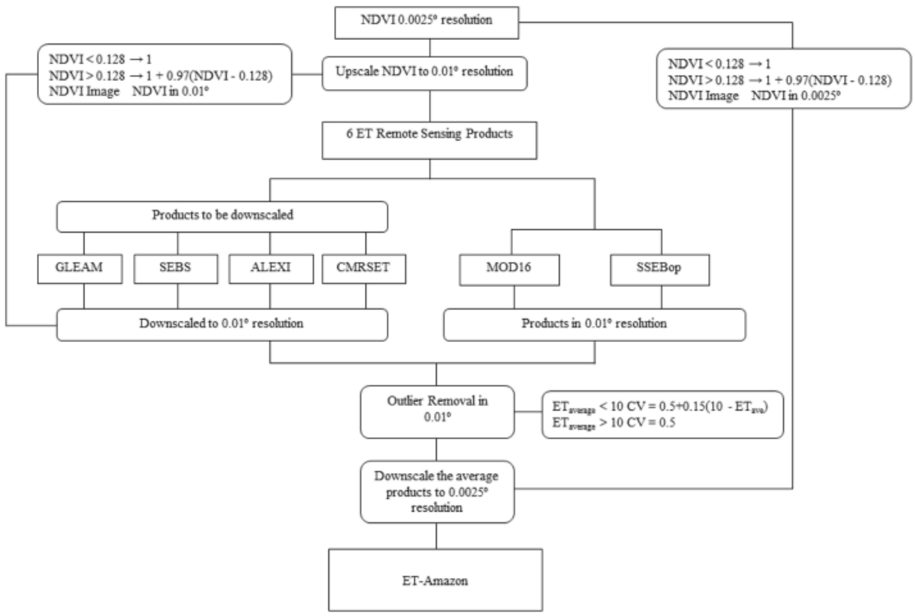


**Fig. 3** Flowchart of the averaging procedure to merge six existing ET products (GLEAM, SEBS, ALEXI, CMRSET, MOD16, and SSEBop) into one product, i.e., ET-Amazon

Eq. (7) applies. Assuming that water storage changes for a period of 10 years (2003 to 2013) can be disregarded, the areal integrated ET can be determined from the water balance as:

$$\mathrm{ET}_y = \int [P(t) - Q(t)]dt \quad (8)$$

$\mathrm{ET}_y$ from the water balance was used to validate the ET-Amazon product for the whole basin at an annual time scale. The annual mean precipitation $P(t)$ obtained by CPRM (2011) from rain gauges was 2460 mm/year for the period 1977 to 2006. Salati et al. (1978) and Ribeiro et al. (1979) acquired similar values for $P(t)$ such as 2478 mm/year. Molinier et al. (1996) recorded a mean discharge ($Q$) of 209.000 m$^3$/s for the Amazon River over the period 1970 to 1990, and Callede et al. (2010) a value of 206.000 m$^3$/s. Normalizing the flow per unit of area amounts to 1080 mm/year. $\mathrm{ET}_y$ can be approximated as 1380 mm/year.

## Results

### Validation of the ET-Amazon product

Figure 4 shows the comparison of time-integrated ET-Amazon values and ET measured by the flux towers. The results shown are accumulated values of ET-Amazon over 2 months or longer, for each of the three closure methods. The maximum period of contiguous measurements is 10 months. The monthly results are presented in Fig. 5. The dashed line in Fig. 4 is the one-to-one reference line (through the origin) between the measured ET and the ET-Amazon. In the plots, the solid line represents the trend line between the measured ET and the ET-Amazon. The direct measurement of latent heat flux (method 1) correlated well with ET-Amazon. Method 1 has the best agreement in terms of root mean square error (slope = 0.900; $R^2$ = 0.985; RMSE 89.7 mm/period). Method 3 reveals a slightly higher coefficient of determination $R^2$ (slope = 1.028; $R^2$ = 0.990; RMSE 62.7 mm/period) and rather importantly, a lower scatter with RMSE of 62.7 mm for the period considered. The lowest bias of 1.003 is found for the residual method 2 (slope = 0.936; $R^2$ = 0.960; RMSE 119.9 mm), but the scatter is higher. The residual of method 2 thus does not require any bias correction, but method 3 has a substantial lower RMSE. Direct measurements of latent heat flux show a lower agreement with the remote sensing data, which many other authors have found as well.

Table 4 shows the validation metrics obtained for each station for integration periods of 2 months or longer. Flux towers K77 and K83 have a short period of overlap and insufficient data points to perform a statistical analysis. The agreement for K34 is the best when method 2 is chosen. K67 shows more agreement for method 3 and BAN for method 1. The table shown in Appendix 4 specifies the months used for each flux station, in summary: BAN (18 months), K34 (14 months), and K67 (20 months). It can be concluded that (i) the energy closure method chosen has impact on the accuracy of the remote sensing results and (ii) every flux station has its

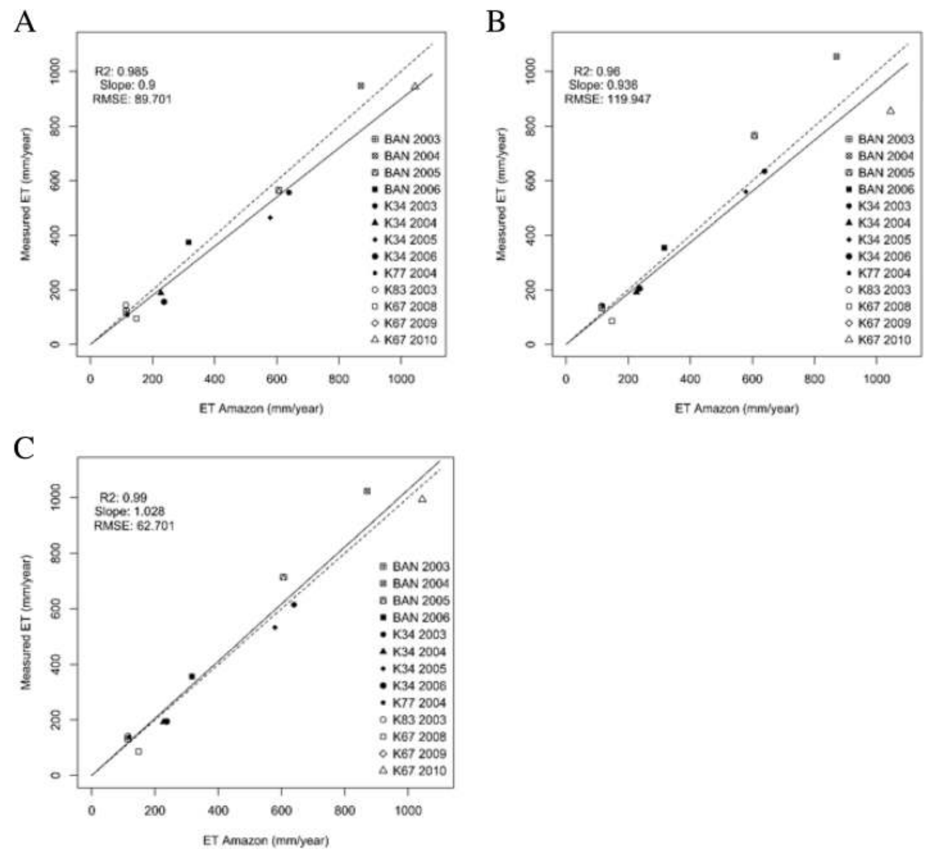


**Fig. 4** Scatter diagram of accumulated ET measured by flux towers plotted against ET-Amazon values for a 2-month or longer integration period, for each of the three ET methods: (1) direct measurements (**a**), (2) the residual of energy balance (**b**), and (3) the Bowen ratio (**c**). The one-to-one line (dashed) and the trend line (solid) are also shown

own closure and correction issues. Validation of ET products in complex environments thus remains to be a challenge, despite the great efforts made by the international LBA community.

Figure 5 and Table 5 represent the ET-Amazon performance against measured ET at monthly time steps. Because of the shorter time interval, the ET range is small. Consequently, the data points are more scattered, and statistical agreements are lower compared to the longer periods. Figure 5 shows that results of the energy balance closure and the Bowen ratio methods have a larger scatter for higher ET values than the directly measured values. The Bowen ratio method showed the best results. ET-Amazon overestimates the measured values in the average range of ± 15 mm/month. The range of ET flux measurements (60 to 140 mm/month) is larger than the range captured by remote sensing (90 to 140 mm/month). It is not understood why the remote sensing data does not encompass low ET values. Perhaps, it is related to the performance of detecting stomatal stress, which for GLEAM and MOD16 is more difficult by their lack of utilizing TIR data.

Although the results of the monthly comparisons are not shown for individual stations, K34 station has the smallest RMSE (13.98 mm/month). The highest correlation was found for K67 ($R^2$ is 0.84). The performance of K34 is less satisfactory ($R^2$ is 0.48 for method 1; $R^2$ is 0.64 for method 2).

Table 5 shows the impacts of footprint dimensions. Smaller footprints provide systematic better agreements, indicating that the area surrounding the flux tower needs special consideration. This was also observed during earlier validation studies of remotely sensed ET fluxes (e.g., Negron Juarez et al. 2008). The findings for K34 seem to disagree with this footprint-related observation because the dense primary forest is more spatially uniform.

Another validation is the comparison between the residual energy and water balance. $ET_y$ was approximated to be 1380 mm/year. There is also a certain margin of error because the longer-term averages of $P$ and $Q$ are not identical. The basin average value of ET-Amazon for the period 2003 to 2013 was 1316 mm/year. The minimum value of ET-Amazon is 1299 mm/year and occurred in the year 2003, while ET-Amazon reached a maximum of 1380 mm/year during 2013. A deviation of − 64 mm (4.6%) between the water and energy balances for

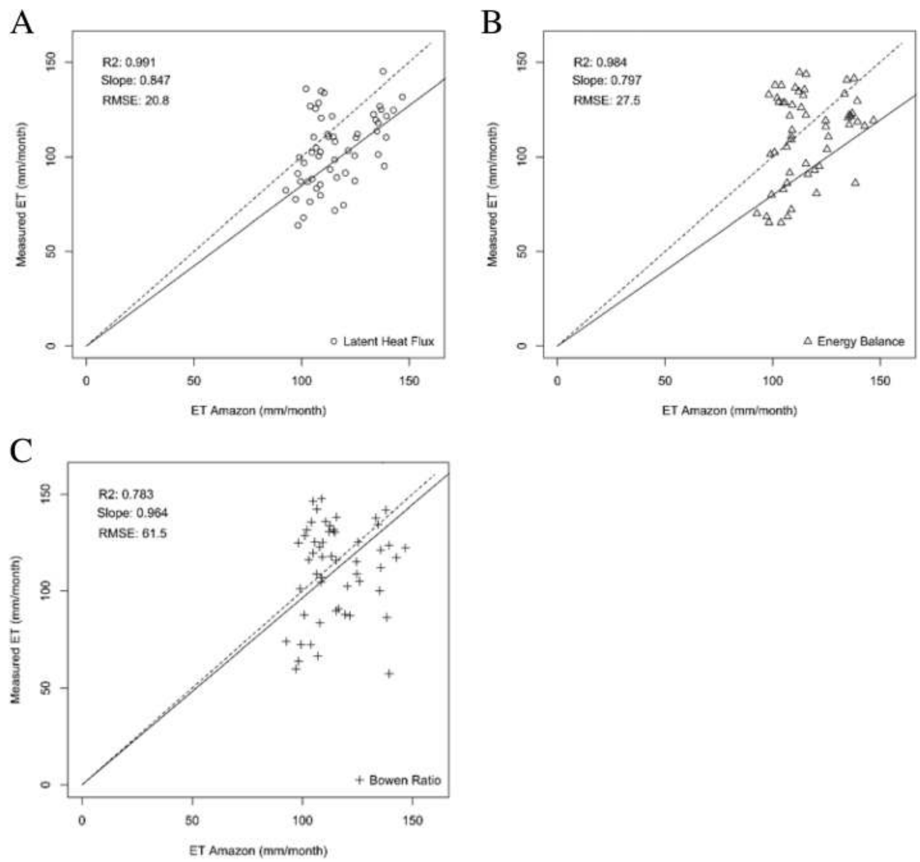


**Fig. 5** Scatter diagram of ET measured monthly at five flux towers, plotted against ET-Amazon from six global energy balance products and the three ET methods: (1) direct measurements (**a**), (2) the residual of energy balance (**b**), and (3) the Bowen ratio (**c**). The one-to-one line (dashed) and the trend line (solid) are also shown

**Table 4** The RMSE and $R^2$ metrics used to validate ET-Amazon for integration periods of 2 months or longer. A footprint of one pixel is considered

| | | | |
|---|---|---|---|
| Direct measurement | | | |
| 250 m | K34 | K67 | BAN |
| RMSE | 83.49 | 147.44 | 52.89 |
| $R^2$ | 0.993 | 0.999 | 0.98 |
| Residual energy balance closure | | | |
| 250 m | K34 | K67 | BAN |
| RMSE | 25.55 | 179.41 | 123.59 |
| $R^2$ | 0.999 | 0.996 | 0.998 |
| Bowen ratio energy balance closure | | | |
| 250 m | K34 | K67 | BAN |
| RMSE | 38.21 | 87.21 | 95.80 |
| $R^2$ | 0.999 | 0.993 | 0.999 |

the entire Amazon is an encouraging finding when considering that methods are entirely different and the water balance observation periods are different. Furthermore, one of the first experiments carried out in Ducke Reserve by Shuttleworth (1988) showed average total evaporation ranging from 87 to 130 mm/month, for the period September 1983 to September 1985, which is in agreement with the mean values found by ET-Amazon for the same site.

Figure 6 shows the ET-Amazon data averaged for the period 2003 to 2013. The ET values vary between 91 mm/year in the high altitudes and 2430 mm/year in the lowland fringe areas of the Guyana's and Surinam. Besides these lowlands, the highest ET rates occur in tropical forests, the Atlantic Coast, and at the foothills of Andes in Bolivia, where the rivers Madre Dios and Beni emerge. The ET features coincide with the higher precipitation rates in the Atlantic Coast, and the lower ET rates occur at the Bolivian and Peruvian rain-shadow slopes of the Andes (ET is 620.4 mm/year). The water divide on the Roraima Mountains in the Andes Cordillera exhibits low ET values due to sparse vegetation with cold climates prevailing at higher altitudes. The

**Table 5** Impact of footprint 250 m × 250 m (6.25 ha) vs. 1750 m × 1750 m (306.25 ha) of flux towers on the performance of ET-Amazon for monthly time steps

| | | | |
|---|---|---|---|
| Direct measurement | | | |
| 250 m × 250 m | K34 | K67 | BAN |
| RMSE | 26.76 | 21.66 | 16.75 |
| $R^2$ | 0.48 | 0.84 | 0.55 |
| 1750 m × 1750 m | K34 | K67 | BAN |
| RMSE | 27.87 | 20.83 | 17.84 |
| $R^2$ | 0.5 | 0.87 | 0.36 |
| Residual energy balance closure | | | |
| 250 m × 250 m | K34 | K67 | BAN |
| RMSE | 14.89 | 22.02 | 24.71 |
| $R^2$ | 0.54 | 0.83 | 0.29 |
| 1750 m × 1750 m | K34 | K67 | BAN |
| RMSE | 13.98 | 27.47 | 23.62 |
| $R^2$ | 0.64 | 0.86 | 0.22 |
| Bowen ratio energy balance closure | | | |
| 250 m × 250 m | K34 | K67 | BAN |
| RMSE | 16.92 | 59.80 | 20.13 |
| $R^2$ | 0.54 | 0.30 | 0.51 |
| 1750 m × 1750 m | K34 | K67 | BAN |
| RMSE | 16.80 | 61.45 | 19.58 |
| $R^2$ | 0.62 | 0.36 | 0.34 |

deforested areas on the south-eastern part of the basin exhibit low ET values as well (720.4 mm/year). Maps with monthly ET values are presented in the Appendix 1. The seasonal trends are presented in Appendix 2.

Monthly average ET of the Amazon is presented in Table 6. The average is 110.1 mm/month, and it varies between 93.7 and 138.2 mm/month. A peak in ET values occurred in January 2013 (138.2 mm/month) followed by a second peak in October 2013 (130 mm/month). January has higher $ET_0$ values than other months, so this peak ET can be climatologically explained. The reason that January shows high ET values is mainly because it is part of the wet season with ample moisture supply which outweighs the effects of a lower $ET_0$, at least for the downstream part of the basin. The minimum ET rates occur in June 2011 (93.7 mm/month) (Fig. 7).

## Comparative analysis

More global scale spatially distributed ET data sets have been developed during recent years. A comparison is needed to demonstrate that ET-Amazon is justified. Three ET products based on ground flux measurements, numerical land surface models, and artificial intelligence (AI) were selected and compared with ET-Amazon: The WAter Cycle Observation Multi-mission Strategy - EvapoTranspiration—WACMOS-ET (Michel et al. 2016), LandFlux-EVAL (Mueller et al. 2013), and Model Tree Ensemble (MTE) (Jung 2009).

The LandFlux-EVAL covers the period 1989 to 2005, with a spatial resolution of 1° × 1° (https://data.iac.ethz.ch/

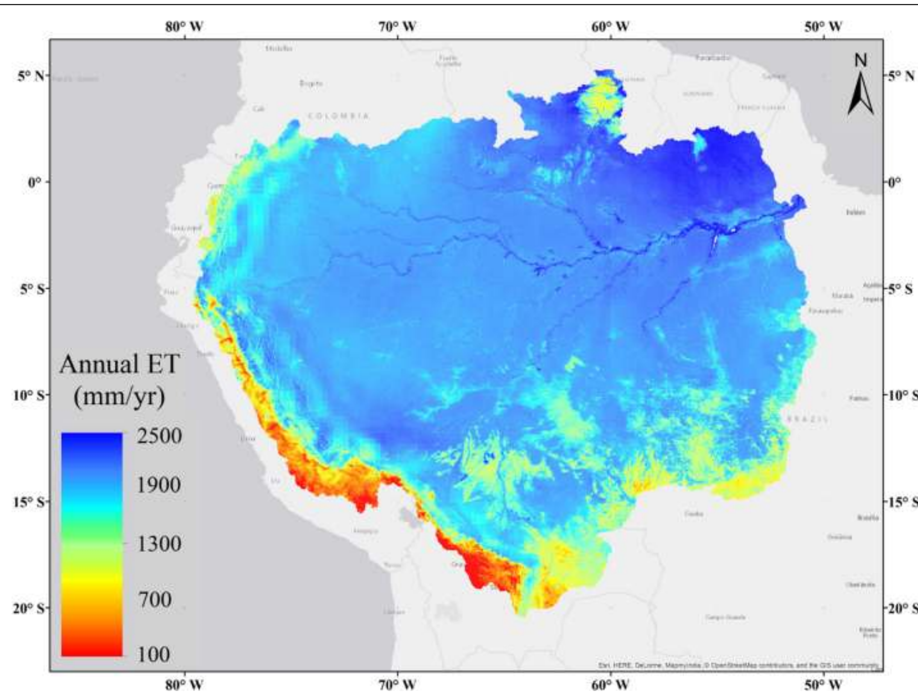


**Fig. 6** Spatial distribution of annual ET over the Amazon basin, averaged for the period 2003 to 2013

**Table 6** Monthly ET values (mm) averaged for the entire Amazon basin

| | 2003 | 2004 | 2005 | 2006 | 2007 | 2008 | 2009 | 2010 | 2011 | 2012 | 2013 |
|---|---|---|---|---|---|---|---|---|---|---|---|
| Jan | 113.5 | 127.2 | 129.3 | 129 | 131.6 | 127.5 | 124.2 | 126.6 | 127.3 | 127.8 | 138.3 |
| Feb | 101.72 | 102.4 | 100.9 | 102.5 | 102.4 | 105 | 99.9 | 101.8 | 100.1 | 104.3 | 101 |
| Mar | 112.2 | 111.7 | 112.2 | 113.5 | 113.6 | 111.9 | 110.4 | 114.9 | 112.4 | 114.6 | 113.2 |
| Apr | 105 | 105 | 104.8 | 105.4 | 107.3 | 104.5 | 104.4 | 106.4 | 105.8 | 106.1 | 107.3 |
| May | 102.5 | 101 | 104.1 | 102.1 | 104.5 | 100.5 | 102.7 | 102.4 | 101.9 | 105.5 | 104.7 |
| June | 93.8 | 94.2 | 94.5 | 95.2 | 95.7 | 94.2 | 93.9 | 93.9 | 93.7 | 97.1 | 97.3 |
| July | 100.4 | 101.2 | 100.6 | 101 | 101.5 | 100.8 | 103.7 | 99.1 | 101.7 | 103.9 | 106.6 |
| Aug | 107.8 | 107.1 | 103.9 | 108.5 | 107 | 107.7 | 110.8 | 104.9 | 107.2 | 108.9 | 115.4 |
| Sep | 111 | 110.3 | 107.3 | 111.6 | 111.4 | 111.3 | 115.7 | 109.2 | 111.9 | 111.7 | 122.2 |
| Oct | 119.5 | 120 | 118.9 | 122 | 118.1 | 118.8 | 122.4 | 118.6 | 120.3 | 122.7 | 130 |
| Nov | 116.9 | 117.7 | 116.3 | 119 | 117.8 | 115.7 | 118.6 | 115.1 | 118.7 | 118.2 | 125.1 |
| Dec | 115 | 114.5 | 113.6 | 116 | 115.1 | 111.7 | 113.2 | 112.8 | 114.2 | 114.6 | 119.1 |
| Total | 1299.3 | 1312.3 | 1306.4 | 1325.8 | 1326.0 | 1309.6 | 1319.9 | 1305.7 | 1315.2 | 1335.4 | 1380.2 |

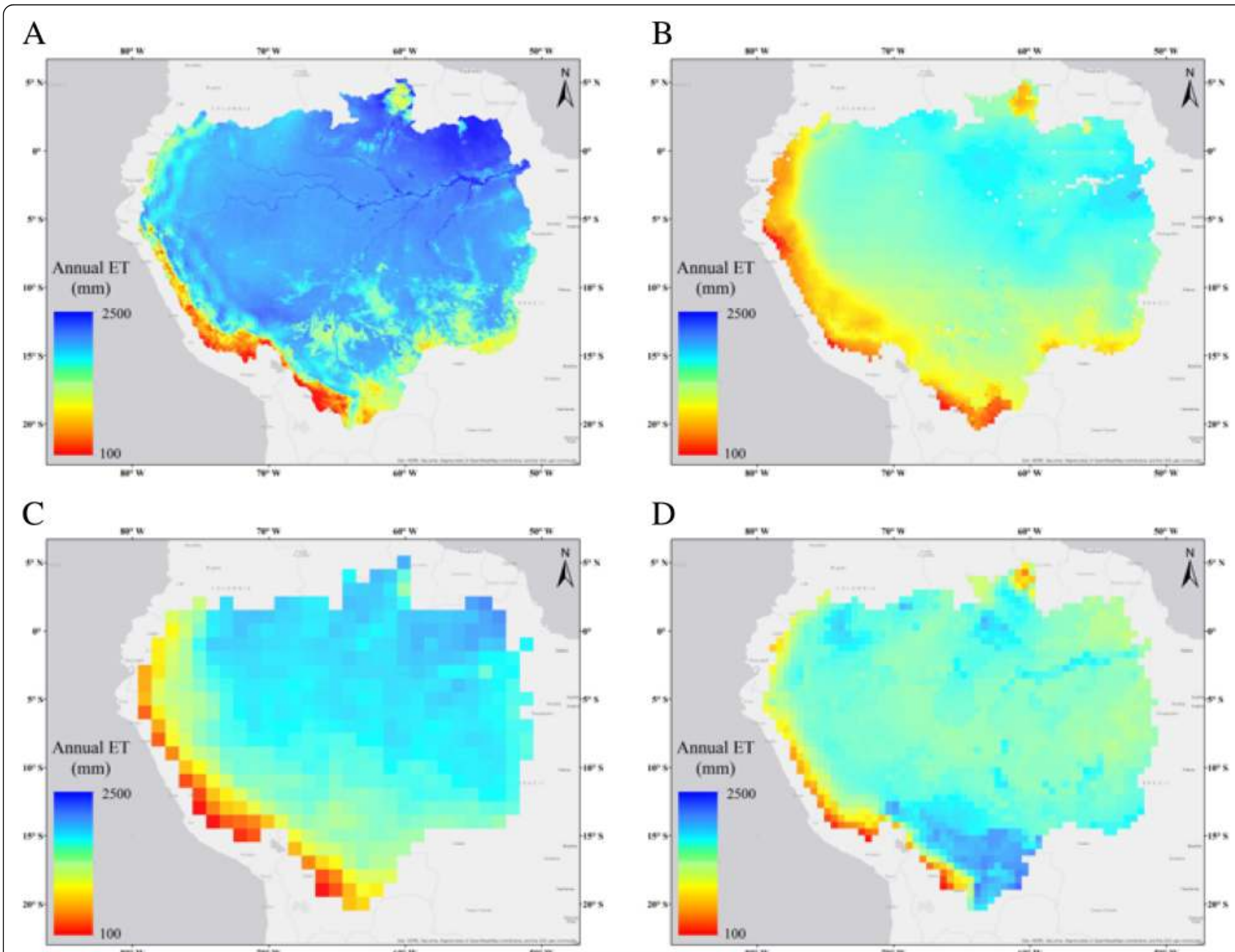


**Fig. 7** Comparison of mean annual ET in the Amazon basin from four ET products: **a** ET-Amazon, **b** WACMOS-ET, **c** LandFlux-EVAL, and **d** MTE

**Table 7** Annual ET statistics for the Amazon River Basin presented by country based on a validated ET-Amazon product

| Country | Mean (mm/year) | Minimum (mm/year) | Maximum (mm/year) | Standard deviation (mm/year) | Area ($km^2$) | ET volume ($km^3$/year) | ET volume (%) |
|---|---|---|---|---|---|---|---|
| Bolivia | 1165.0 | 45.4 | 2349.9 | 265.8 | 714,255.6 | 832.1 | 10.7 |
| Brazil | 1375.0 | 249.1 | 2577.8 | 157.7 | 3,681,897.3 | 5062.6 | 65.2 |
| Colombia | 1324.5 | 694.6 | 1800.1 | 90.7 | 342,154.2 | 453.1 | 5.8 |
| Ecuador | 1230.2 | 523.6 | 1751.1 | 138.0 | 132,230.8 | 162.6 | 2.1 |
| Guyana | 1318.7 | 674.1 | 1858.6 | 228.3 | 12,599.7 | 16.6 | 0.2 |
| Peru | 1205.7 | 104.2 | 1922.3 | 277.7 | 966,330.7 | 1165.1 | 15.0 |
| Venezuela | 1429.7 | 854.6 | 1785.6 | 55.8 | 52,962.1 | 75.7 | 1.0 |

landflux/). The MTE product (Jung et al. 2010) is upscaled from the database of the FLUXNET. The MTE ran for a longer period, from 1982 to 2011, spatially distributed on a 0.5° × 0.5° grid (https://www.bgc-jena.mpg.de/geodb/projects/Home.php). The WACMOS-ET Project has a better spatial resolution of 0.25° × 0.25°, for the period 2005 to 2007. The WACMOS-ET product is a combination of LandFlux-EVAL and MTE, and thus expected to be superior. For more background information on these products, the reader is referred to the original papers.

The ET obtained by the MTE product (Jung 2009) varies between a rate of 2.7 and 9.5 mm/day, with a mean annual ET of 1153 mm/year. The LandFlux-EVAL ET varies between 3.3 and 10.0 mm/day, with a mean annual ET of 1172 mm/year. The ET mean value for the WACMOS-ET is with 1087 mm/year, even lower. Hence, the mean values are significantly lower than $ET_y$ of 1380 mm/year found from the water balance. The statistics for WACMOS-ET, LandFlux-EVAL, and MTE show that the minimum values are reasonable, but the maximum values are far off and occur in geographic areas where you do not expect them. Global ET products based on an upscaling procedure using flux measurements from other regions should therefore be treated with caution.

Except for the MTE results, the comparison demonstrates that the spatial ET patterns towards the north-east of the Amazon basin are similar. The Andes and the natural fields surrounding the three borders of Brazil, Guyana, and Venezuela show similarity for all four products. Although the LandFlux-EVAL product has the coarsest resolution, the spatial features best comply with ET-Amazon, indicating that the Guyana's have the largest ET.

### ET-Amazon breakdown by country

The ET-Amazon values shown in Fig. 6 can be parsed by sub-basins (e.g., Maeda et al. 2017), land use, and by country. A small portion of the Amazon territory (10%) is located within Colombia, Ecuador, Venezuela, and Guyana. Brazil, Bolivia, and Peru together occupy 90.8% of the basin area. For the purpose of managing the transboundary Amazon River, it is of essence to know how consumptive use is broken down by country. The breakdown of total volumetric ET (7060 $km^3$/year) for the basin is shown in Table 7. Figure 8 shows box-plots of the actual ET per month, by country. The main feature for the years analyzed is that intra-variability is minimal. The main reason for the low seasonal variation is the compensating effects of soil moisture and evaporative demand of the atmosphere in combination with the presence of green leaves. Root zone soil moisture availability is a constraint during the dry season, while solar radiation and reference $ET_0$ reach its maximum (see Fig. 2). Radiation controls the evaporation process during the wet season, when soils can be assumed to be at field capacity. Moisture is stored in the vadose zone for annual cycles and making water available throughout the entire year. The deep root zone of forests acts as a large buffer and provides storage of water for the vegetation (Wang-Erlardson et al. 2016). During elevated precipitation rates, soil moisture storage is replenished by recharge and released again during dry seasons or during dry years. This regulating mechanism is responsible for the quasi-constant flux rates.

Bolivia has the lowest ET (1165 mm/year) while Venezuela shows the highest ET value (1430 mm/year). Bolivia and Peru show the largest intra-annual variability. The latter can be attributed to rainfall and weather variability yielding a certain behavior of soil moisture dynamics. Volume wise, the picture is entirely different. Table 7 shows that Brazil evaporates 5062.6 $km^3$/year (65.2%), followed by Peru (1165.1 $km^3$/year or 15.0%), and Bolivia (832.1 $km^3$/year or 10.7%).

Table 8 shows the relationship between land cover and ET by trimester. The ET values are the lowest for sparse vegetation and highest for dense forested areas. The most common land use and land cover category is closed to open broadleaved evergreen or semi-deciduous forest. Closed to open grassland evaporates 925 mm/year, being significantly less than closed forests (1370 to 1380 mm/year). Land use changes from forest to field, to agricultural, to grazing, and to secondary forests (capoeira), all decrease the ET of the Amazon. According to Tollefson (2016), deforestation across the Amazon River

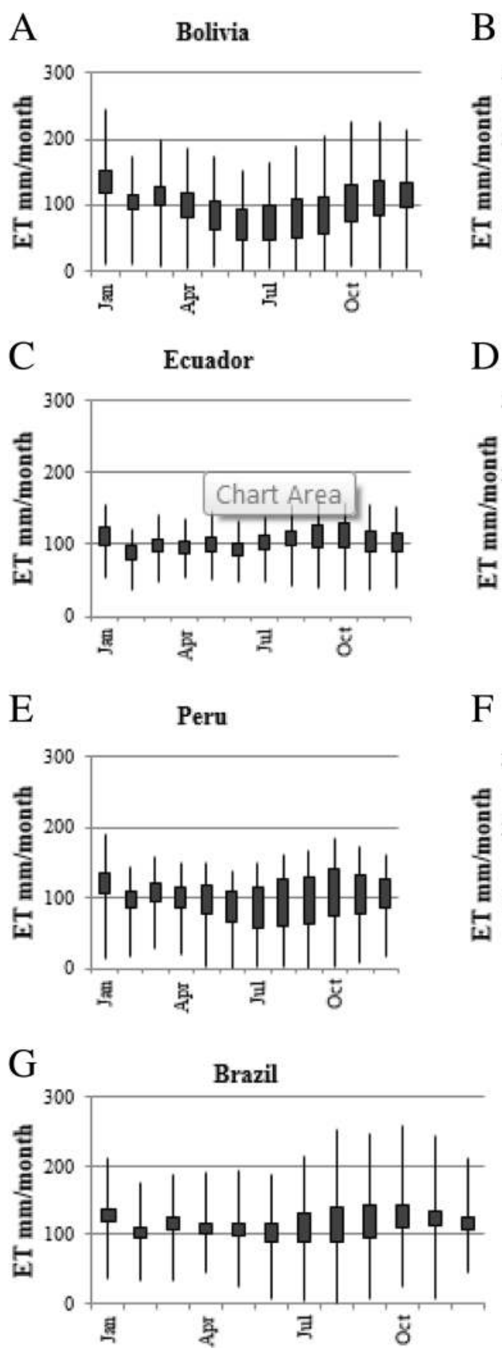


**Fig. 8** Monthly ET rates for Bolivia (**a**), Colombia (**b**), Ecuador (**c**), Guyana (**d**), Peru (**e**), Venezuela (**f**), and Brazil (**g**). The mean values and the standard deviations are plotted

Basin has increased since 2008. Thus, reduction in ET is a direct consequence of deforestation, something also noted by Nobre (2014). A land cover change of 100,000 $km^2$ from closed forest to pasture implies a reduction of 4500 $km^3$/year of water transfer into the atmosphere. A lower regional ET not only affects rainfall, it will also increase the river flow and flood risk. It is thus essential to understand ET by land cover type, and this paper comprehensively describes this situation for the giant and largely unknown Amazon basin.

## Summary and conclusions

ET-Amazon is a new remote sensing evapotranspiration product that facilitates the description of land surface hydrological processes in one of the world's largest river systems that is still poorly understood. ET-Amazon was

**Table 8** Mean seasonal ET (and standard deviation) from ET-Amazon parsed by land cover and land use class (http://due.esrin.esa.int/page_globcover.php)

| Land cover | Area ($km^2$) | Area (%) | JFM (mm) | AMJ (mm) | JAS (mm) | OND (mm) | Annual (mm/year) |
|---|---|---|---|---|---|---|---|
| Sparse vegetation | 10,889.6 | 0.2 | 76.4 (13.9) | 40.4 (18.4) | 25.8 (16.9) | 48.2 (20.5) | 572.1 |
| Mosaic grassland/forest-shrubland | 6033.7 | 0.1 | 76.7 (12.1) | 38.4 (13.7) | 21.8 (12.6) | 44.3 (15.7) | 543.7 |
| Artificial areas | 753.0 | 0.1 | 82.0 (18.9) | 58.5 (27.5) | 52.2 (36.4) | 71.3 (32.4) | 792.0 |
| Bare areas | 6560.1 | 0.1 | 85.0 (17.4) | 57.1 (26.0) | 46.7 (32.3) | 68.1 (30.9) | 770.5 |
| Closed to open grassland | 76,620.0 | 1.3 | 93.1 (16.9) | 71.9 (18.1) | 60.4 (31.4) | 83.0 (25.8) | 924.9 |
| Mosaic forest-shrubland/grassland | 19,498.7 | 0.3 | 93.9 (18.2) | 70.5 (25.7) | 58.2 (34.4) | 79.8 (30.1) | 907.0 |
| Closed to open shrubland | 249,490.8 | 4.3 | 95.3 (19.3) | 74.0 (24.5) | 62.5 (35.1) | 86.1 (27.8) | 953.6 |
| Open broadleaved deciduous forest | 308.8 | 0.1 | 104.4 (15.7) | 65.9 (19.4) | 45.5 (23.1) | 81.3 (21.0) | 891.1 |
| Rainfed croplands | 943.7 | 1.1 | 108.5 (12.3) | 70.9 (16.1) | 44.0 (21.3) | 91.2 (19.5) | 943.7 |
| Closed to open vegetation regularly flooded | 97,001.6 | 1.7 | 109.8 (10.0) | 93.9 (13.7) | 96.8 (26.7) | 113.7 (14.3) | 1242.7 |
| Mosaic croplands/vegetation | 233,958.2 | 4.0 | 109.9 (11.8) | 88.4 (17.8) | 73.7 (28.3) | 104.2 (17.9) | 1128.7 |
| Mosaic vegetation/croplands | 87,718.3 | 1.5 | 111.5 (12.9) | 81.6 (18.1) | 64.2 (29.3) | 99.7 (19.2) | 1070.9 |
| Closed to open broadleaved forest regularly flooded (fresh-brackish water) | 176,586.0 | 3.0 | 115.0 (7.2) | 105.6 (7.6) | 118.1 (16.6) | 122.4 (9.0) | 1383.1 |
| Closed to open broadleaved evergreen or semi-deciduous forest | 4,690,468.8 | 80.1 | 116.4 (8.1) | 105.4 (9.2) | 114.7 (18.5) | 122.2 (10.9) | 1376.0 |
| Closed broadleaved deciduous forest | 51,243.9 | 1.0 | 117.2 (10.0) | 74.1 (17.1) | 57.4 (19.0) | 98.5 (16.5) | 1041.5 |
| Closed broadleaved forest permanently flooded (saline-brackish water) | 53.5 | 0.1 | 121.3 (8.9) | 99.1 (11.7) | 99.5 (17.0) | 123.6 (10.9) | 1330.1 |

created by linear averaging of six existing ET products. This is a straightforward but effective methodology to average out uncertainties related to one single ET model. The data-poor environment did not permit development of a more sophisticated ensemble ET prediction using a priori knowledge.

The validation was performed by comparing results with measured ET from flux towers. The average energy balance closure varied between 86 and 116%, which is acceptable by the international scientific community, but implies practically that all validation exercises are somewhat weak. Without any calibration, the correlation coefficient, slope, and RMSE were 0.974, 1.003, and 91.7 mm for longer periods (2 to 10 months), respectively. For monthly periods, 0.991, 0.847, and 20.8 mm were found. The time-integrated ET flux measurements had a bias correction of 0.3% only without any a priori calibration of ET-Amazon. ET-Amazon was also verified at river basin scale and showed a 4.6% difference only. The congruency with local flux tower measurements and basin scale water balance data suggests that the ET maps and their statistics by country and land use are reliable. It is therefore concluded that this new remote sensing product is justifiable.

The results of the ET-Amazon product were also compared with three other state-of-art ET products often used for ecological and hydrological studies. Their ET values were systematically underestimated, they had a coarser resolution, and the spatial pattern was not obvious. One plausible factor for the poor performance is that training on flux measurements from mainly Europe and the USA cannot be used out of its geographical-specific context.

One limitation of ET-Amazon is that it only provides monthly values and does not indicate which ET products were used for the final data set. The authors have checked that often most ET models form the basis of the final ET layer.

The ET-Amazon has a spatial resolution of 0.0025°, and it was developed with data from January 2003 to December 2013. It is a high-resolution product that makes it possible to analyze actual ET at local, up to river basin scale, as well as by country and by land cover. The estimation of evapotranspiration from remote sensing empowers the implementation of frameworks such as water accounting which can lead to the improvement of local river flow estimates in ungauged basins and water management practices in the Amazon River Basin. This study shows the amount of water consumed by agro-ecological processes for each government, local water authorities, and *non-governmental organizations* (NGOs) residing in the Amazon basin. The use of ET-Amazon will greatly improve the prediction of the impacts of land use changes on rainfall, river flow, and floods. The data can be downloaded from www.wateraccounting.org.

## Appendix 1

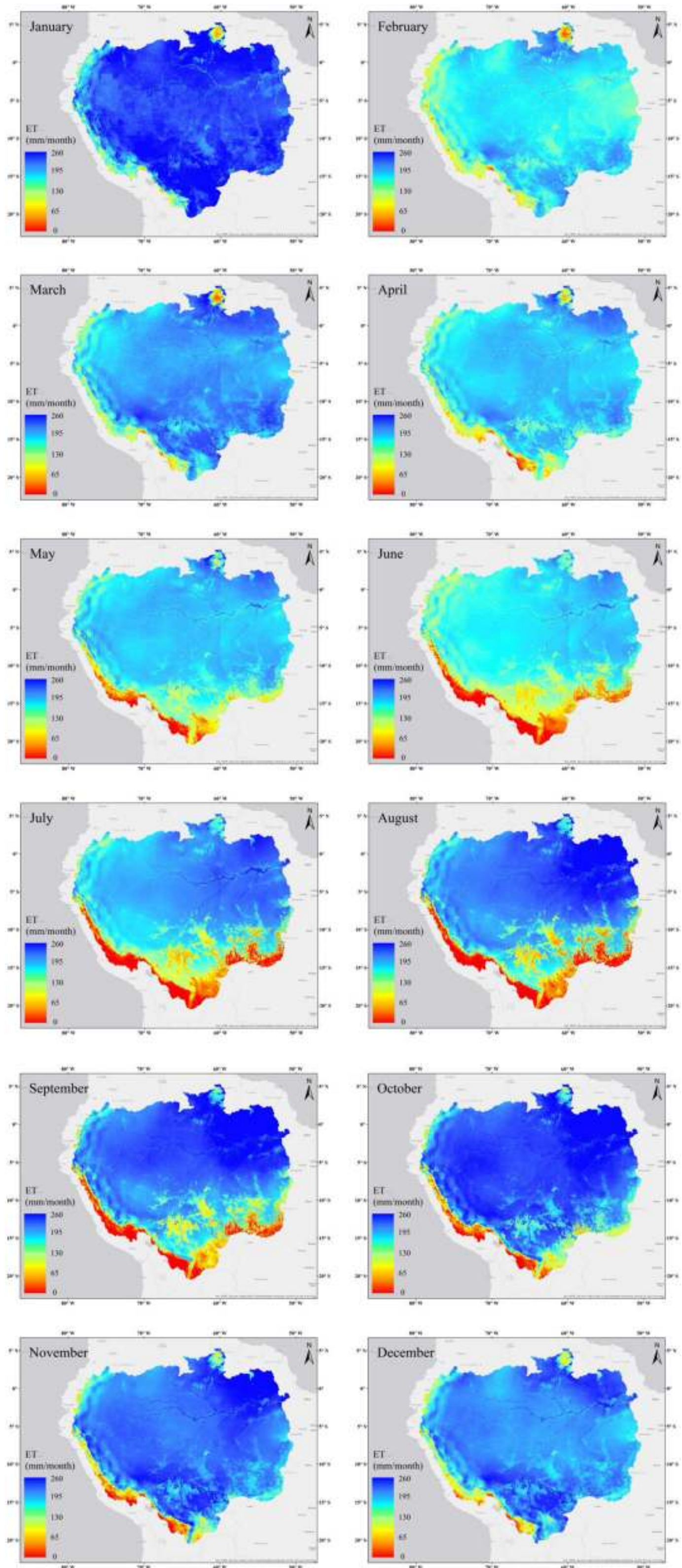


**Fig. 9** Monthly ET over the period 2003 to 2013 based on ET-Amazon

## Appendix 2

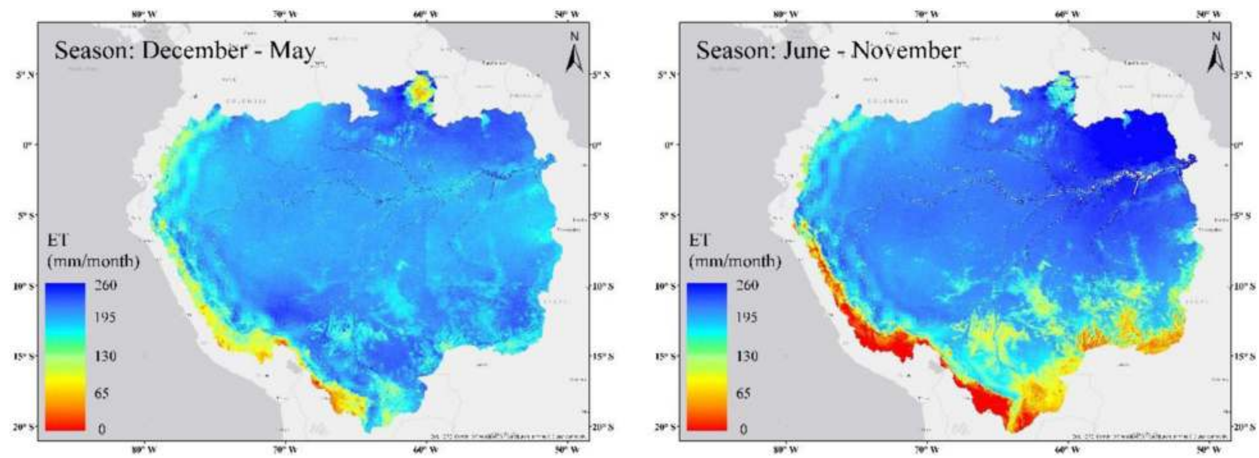


**Fig. 10** Seasonal ET over the period 2003 to 2013 based on ET-Amazon

## Appendix 3

**Table 9** Sources of the ET products

| Product | Source |
| --- | --- |
| GLEAM | hydras.ugent.be |
| SEBS | ftp://ftp.wateraccounting.unesco-ihe.org/WaterAccounting/Data_Satellite/Evaporation/SEBS/SEBS/ |
| ALEXI | ftp://ftp.wateraccounting.unesco-ihe.org/WaterAccounting/Data_Satellite/Evaporation/ALEXI/World/ |
| CMRSET | ftp://ftp.wateraccounting.unesco-ihe.org/WaterAccounting/Data_Satellite/Evaporation/CMRSET/Global/ |
| MOD16 | http://files.ntsg.umt.edu/data/NTSG_Products/MOD16/MOD16A2_MONTHLY.MERRA_GMAO_1kmALB |
| SSEBOP | https://edcintl.cr.usgs.gov/downloads/sciweb1/shared/fews/web/global/monthly/eta/downloads/ |
| NDVI | https://e4ftl01.cr.usgs.gov/MOLT/MOD13Q1.006/ |

## Appendix 4

**Table 10** Yearly validation of the ET-Amazon, and years used

| Flux tower code | Years | Months used per year | ET-Amazon (mm/year) | Flux tower (mm/year) direct measurement | Flux-tower (mm/year) energy balance closure | Flux tower (mm/year) Bowen ratio |
|---|---|---|---|---|---|---|
| BAN | 2003 | 1 | 114.8 | 121.5 | 132.6 | 131.7 |
| BAN | 2004 | 8 | 870.6 | 948.5 | 1054.5 | 1023.1 |
| BAN | 2005 | 6 | 606.2 | 565 | 765.9 | 713.6 |
| BAN | 2006 | 3 | 316.4 | 374.7 | 354.4 | 356.7 |
| K34 | 2003 | 5 | 639 | 556.3 | 634.3 | 614.4 |
| K34 | 2004 | 2 | 226.6 | 188.8 | 192.1 | 192 |
| K34 | 2005 | 5 | 578.9 | 464.1 | 559.1 | 531.8 |
| K34 | 2006 | 2 | 237.1 | 156.8 | 205.4 | 194.4 |
| K77 | 2004 | 1 | 118.5 | 108.1 | 143.6 | 138.4 |
| K83 | 2003 | 1 | 114.2 | 145.1 | 141.4 | 141.8 |
| K67 | 2008 | 1 | 147.9 | 95.1 | 86.1 | 86.3 |
| K67 | 2009 | 10 | 1169.7 | 942.4 | 883.1 | 1200.4 |
| K67 | 2010 | 9 | 1044.7 | 944.6 | 854.9 | 993.1 |

**Acknowledgements**
This study was financially supported by the CPRM - The Geological Survey of Brazil, and CNPq - COIAM /HIDRO-EX, project number: 211902/2013-6. We would like to thank LBA staff for data sharing and support, especially MSc Marta de Oliveira Sá (INPA), MSc Leila do Socorro Monteiro Leal (INPA), Dr. Alessandro Carioca de Araújo (EMBRAPA - Amazônia Oriental), Dra Renata Gonçalves Aguiar (UNIR/RO), Ms. Jayne Soares Martins do Nascimento (UNIR/RO), Mr. Jonatas Schweigert (UNIR/RO), and our real thanks for all support and patience to Dra Elisângela Broedel (INPE), and Dr. Celso von Randow (INPE). For the valuable contribution to validate the ET-Amazon and share the dataset of the respective projects: Dr. Carlos Jimenez from WACMOS-ET, Dr. Martin Jung from the MTE, and Dr. Martin Hirschi from LandFlux-EVAL.

**Funding**
CNPq - COIAM /HIDRO-EX (211902/2013-6); CPRM - Geological Survey of Brazil.

**Availability of data and materials**
Please contact author for data requests.

**Authors' contributions**
All authors have contributed directly to this research. All authors read and approved the final manuscript.

**Consent for publication**
Not applicable.

**Competing interests**
The authors declare that they have no competing interests.

## Publisher's Note

Springer Nature remains neutral with regard to jurisdictional claims in published maps and institutional affiliations.

**Author details**
[1]IHE Delft Institute for Water Education, Westvest 7, Delft 2611 AX, Netherlands. [2]TU Delft, Delft, Netherlands. [3]CPRM - Geological Survey of Brazil, Rio de Janeiro, Brazil. [4]World Bank, Washington, D.C., USA.

Received: 23 October 2018 Accepted: 21 January 2019
Published online: 15 February 2019

**References**

Anderson MC, Norman JM, Mecikalski JR, Otkin JA, Kustas WP (2007) A climatological study of evapotranspiration and moisture stress across the continental United States based on thermal remote sensing: 1. Model formulation. Journal of Geophysical Research Atmospheres 112(10):1–17

Araújo AC, Nobre AD, Kruijt B, Elbers JA, Dallarosa R, Stefani P, von Randow C, Manzi AO, Culf AD, Gash JHC, Valentini R, Kabat P (2002) Comparative measurements of carbon dioxide fluxes from two nearby towers in a central Amazonian rainforest: the Manaus LBA site. J Geophys Res 107

Bastiaanssen, W.G.M. and S. Ali. (2003). A new crop yield forecasting model based on satellite measurements applied across the Indus Basin, Pakistan. Agri Ecol Environ, 94(3):321–340

Bastiaanssen WGM, Chandrapala L (2003) Water balance variability across Sri Lanka for assessing agricultural and environmental water use. Agric Water Manag 58(2):171–192

Bastiaanssen, Wim G. M., Mobin-ud-Din Ahmad, and Yann Chemin. 2002. Satellite surveillance of evaporative depletion across the Indus Basin. *Water Resources Research* 38(12):9–1–9–9

Braga B, Salati E, de Lemos HM (1999) Sustainable water-resources development of the Amazon basin. In: Biswas AK (ed) Management of Latin American River Basins: Amazon, Plata, and São Francisco. UNU, Tokyo New York Paris, pp 3–48

Callede, J., Cochonneau, G., Ronchail, J., Alves, V., Guyot, J., Guimaraes, V., and De Oliveira, E. (2010) Les apports en eau de l'Amazone a l'Ocean Atlantique. Revue des Sciences de l'eau, 23:247–273

Costa MH, Foley JA (1999) Trends in the hydrologic cycle of the Amazon Basin. J Geophys Res 104(D12):14189

CPRM. 2011. "Levantamento Da Geodiversidade - Projeto Atlas Pluviométrico Do Brasil - Isoetas Anuais Médias Período 1977 a 2006." : 2006

da Rocha HR, Manzi AO, Shuttleworth J (2009) Evapotranspiration. In: Gash J, Keller PSDM, Bustamante M (eds) Amazonia and Global Change. American Geophysical Union, Washington, D. C., pp 261–272

Davidson EA, de Araújo AC, Artaxo P, Balch JK, Brown IF, Bustamante C, Mercedes M, Coe MT, Defries RS, Keller M, Longo M, Munger JW, Schroeder W, Soares-Filho BS, Souza CM, Wofsy SC (2012) The Amazon Basin in transition. Nature 481(7381):321–328

de Gonçalves, L G G, N. Restrepo-Coupe, H.R. da Rocha, S.R. Saleska, and R. Stockli. 2013. "LBA-ECO CD-32 LBA Model Intercomparison Project (LBA-MIP) Forcing Data"

Duan Q, Gupta V (1992) Effective and efficient global optimization for conceptual rainfall-runoff models. Water Resour Res 28(4):1015–1031
Fisch G, Gash JHC, Nobre CA, Shuttleworth WJ (2008) Pre-LBA Amazonian Region Micrometeorological Experiment (ARME) Data
Fisch, Gilberto, José Marengo, and C. a Nobre. 1998. Uma Revisão Geral Sobre O Clima Da Amazônia. Acta Amazon 28:101–126
Gash, J H C, C A Nobre, J M Roberts, and R L (eds.) (1996) Amazonian Deforestation and Climate. Institute of Hydrology Victoria Crowmarsh Gifford, Wallingford OX10 8BB, United Kingdom.
Gloor M, Brienen RJW, Galbraith D, Feldpausch TR, Scheongart J, Guyot J-L, Espinoza JC, Lloyd J, Phillips OL (2013) Intensification of the Amazon hydrological cycle over the last two decades. Geophys Res Lett 40(9): 1729–1733
Guerschman JP, Van Dijk AIJM, Mattersdorf G, Beringer J, Hutley LB, Leuning R, Pipunic RC & Sherman (2009) Scaling of potential evapotranspiration with MODIS data reproduces flux observations and catchment water balance observations across Australia. J Hydrol 369(1–2):107–119
Harriss RC (2008) Pre-LBA ABLE-2A and ABLE-2B Expedition Data
Hofste RW (2014) Comparative analysis among near-operational evapotranspiration products for the Nile Basin based on earth observations. Delft University of Technology, Delft, The Netherlands, Master thesis
Jia L, Shang H, Menenti M (2010) Vegetation response to upstream water yield in the Heihe river by time series analysis of MODIS data. Hydrol Earth Syst Sci Discuss 7(4):4177–4218
Jung M, Reichstein M, Bondeau A (2009) Towards global empirical upscaling of FLUXNET eddy covariance observations: validation of a model tree ensemble approach using a biosphere model. Biogeosci Discuss 6(3):5271–5304
Jung M, Reichstein M, Ciais P, Seneviratne S, Sheffield J, Goulden ML, Bonan GB, Cescatti A, Chen J, de Jeu R, Dolman AJ, Eugster W, Gerten D, Gianelle D, Gobron N, Heinke J, Kimball J, Law BE, Montagnani L, Mu Q, Mueller B, Oleson K, Papale D, Richardson AD, Roupsard O, Running S, Tomelleri E, Viovy N, Weber U, Williams C, Wood E, Zaehle S, Zhang K (2010) Recent decline in the global land evapotranspiration trend due to limited moisture supply. Nature 467(7318):951–954
Karimi P, Bastiaanssen WGM (2015) Spatial evapotranspiration, rainfall and land use data in water accounting - Part 1: Review of the accuracy of the remote sensing data. Hydrol Earth Syst Sci 19(1):507–532
Karimi P, Bastiaanssen WGM, Molden D, Cheema MJM (2013) Basin-wide water accounting based on remote sensing data: an application for the Indus Basin. Hydrol Earth Syst Sci 17(7):2473–2486
Kustas WP, French AN, Hatfield JL, Jackson TJ, Moran MS, Rango A, Ritchie JC, Schmugge TJ (2003) Remote sensing research in hydrometeorology. Photogramm Eng Remote Sens 69(6):631–646
Liu W, Wang L, Zhou J, Li Y, Sun F, Fu G, Li X, Sang Y-F (2016) A worldwide evaluation of basin-scale evapotranspiration estimates against the water balance method. J Hydrol 538:82–95
Lopes AV, Chiang JCH, Thompson SA, Dracup JA (2016) Trend and uncertainty in spatial-temporal patterns of hydrological droughts in the Amazon Basin. Geophys Res Lett 43(7):3307–3316
Malhi Y, Roberts JT, Betts RA, Killeen TJ, Li W, Nobre CA (2015) Climate change, deforestation, and the fate of the Amazon. Science 319:169–172
Marengo JA (2006) On the hydrological cycle of the Amazon Basin; a historical review and current state-of-the-art. Revista Brasileira de Meteorologica 21:1–19
Marengo JA, Espinoza JC (2016) Extreme seasonal droughts and floods in Amazonia: causes, trends and impacts. Int J Climatol 36(3):1033–1050
Marques J, Salati E, Santos JM (1980) Cálculo Da Evapotranspiração Real Na Bacia Amazônica Através Do Método Aerológico. Acta Amazon 10(2):357–361
Michel D, Jiménez C, Miralles DG, Jung M, Hirschi M, Ershadi A, Martens B, McCabe MF, Fisher JB, Mu Q, Seneviratne SI, Wood EF, Fernández-Prieto D (2016) The WACMOS-ET project - Part 1: Tower-scale evaluation of four remote-sensing-based evapotranspiration algorithms. Hydrol Earth Syst Sci 20(2):803–822
Miralles DG, Holmes TRH, De Jeu RAM, Gash JH, Meesters AGCA, Dolman AJ (2011) Global land-surface evaporation estimated from satellite-based observations. Hydrol Earth Syst Sci 15(2):453–469
Mohamed YA, van den Hurk BJJM, Savenije HHG, Bastiaanssen WGM (2005) Hydroclimatology of the Nile: results from a regional climate model. Hydrol Earth Syst Sci 9(3):263–278
Molinier MJ-L Guyot, Eurides De Oliveira, and Valdemar Guimaraes (1996) Les Régimes Hydrologiques de L â€™ Amazone et de Ses Affluents. L'hydrologie tropicale: géoscience et outilpourle développement (238)
Mu Q, Zhao M, Running SW (2011) Improvements to a MODIS global terrestrial evapotranspiration algorithm. Remote Sens Environ 115(8):1781–1800
Mueller B, Hirschi M, Jimenez C, Ciais P, Dirmeyer PA, Dolman AJ, Fisher JB, Jung M, Ludwig F, Maignan F, Miralles DG, McCabe MF, Reichstein M, Sheffield J, Wang K, Wood EF, Zhang Y, Seneviratne SI (2013) Benchmark products for land evapotranspiration: LandFlux-EVAL multi-data set synthesis. Hydrol Earth Syst Sci 17(10):3707–3720
Nagler PL, RK Scott C, Westenburg JRC, Glenn E, Huete A, Scott R, Cleverly J, Glenn E (2005) Evapotranspiration on western US rivers estimated using the Enhanced Vegetation Index from MODIS and data from eddy covariance and Bowen ratio flux towers. J Hydrol 8(1–3):1123–1129
Negron Juarez RI, Goulden ML, Myneni RB, Fu R, Bernardes S, Gao H, Nobre C, Goulden M, Wofsy SC (2008) An empirical approach to retrieving monthly evapotranspiration over Amazonia. Int J Remote Sens 29(24):7045–7063
Nobre AD (2014) The future climate of Amazonia scientific assessment report
Nobre CA, Sampaio G, Borma LS, Castilla-Rubio JC, Silva JS, Cardoso M (2016) Land-use and climate change risks in the Amazon and the need of a novel sustainable development paradigm. Proceedings of the National Academy of Sciences, 113:10759–68
Nobre CA, Borma LDS (2013) Secas Na Amazônia: Causas E Consequências
Paca, Victor Hugo da Motta, Meiguins de Lima, A.M., de Azambuja, A.M.S., Fortes, J.D.N., de Souza, J.E.F. (2011) Condições de Operação E Implantação de Estaçòes Da Rede Hidrométrica Da Amazônia Oriental - Estado Do Pará. In *XIX Simpósio Brasileiro de Recursos Hídricos*:1–14
Pelgrum H, Bastiaanssen WGM (1996) An intercomparison of techniques to determine the area-averaged latent heat flux from individual in situ observations: a remote sensing approach using the European field experiment in a desertification-threatened area data. Water Resour Res 32(9): 2775–2786
Poortinga A, Bastiaanssen W, Simons G, Saah D, Senay G, Fenn M, Bean B, Kadyszewski J (2017) A self-calibrating runoff and streamflow remote sensing model for ungauged basins using open-access earth observation data. Remote Sens 9(1):1–14
Prior A (2016) WA + as a technical tool for transboundary water governance: the potential of satellite data for water accounting in ungauged basins. Vrije Universiteit Brussel, Belgium, Master Thesis
Ramoelo A, Majozi N, Mathieu R et al (2014) Validation of global evapotranspiration product (MOD16) using flux tower data in the African savanna, South Africa. Remote Sens 6(8):7406–7423. https://doi.org/10.3390/rs6087406
Restrepo-Coupe N, da Rocha HR, Hutyra LR, da Araujo AC, Borma LS, Christoffersen B, Cabral OMR, de Camargo PB, Cardoso FL, da Costa ACL, Fitzjarrald DR, Goulden ML, Kruijt B, Maia JMF, Malhi YS, Manzi AO, Miller SD, Nobre AD, von Randow C, Sá LDA, Sakai RK, Tota J, Wofsy SC, Zanchi FB, Saleska SR (2013) What drives the seasonality of photosynthesis across the Amazon basin? A cross-site analysis of eddy flux tower measurements from the Brasil flux network. Agric For Meteorol 182–183:128–144
Ribeiro MNG, Villa-Nova NA (1979) Estudos climáticos da Reserva Ducke, Manaus, AM. III. Evapotranspiração. Acta Amazônia 9:305–309
Rouse JW, Haa RH, Schell JA, Deering DW (1973) Monitoring vegetation systems in the Great Plains with ERTS, Third ERTS Symposium, NASA SP-351 I, pp 309–317
Salati E, Marquez J, Molion LC (1978) Origem e distribuição das chuvas na Amazonia. Interciencia 3:200–205
Salati E (1987) The forest and the hydrological cycle. In The geophysiology Amazonia: vegetation and climate interactions, ed. R.E. Dickison. Washington, D. C.: Wiley, 432–60
Salati E, Dall'Olio A, Matsui E, Gat JR (1979) Recycling of water in the Amazon basin: an isotopic study. Water Resour Res 15(5):1250–1258
Saleska SR, da Rocha HR, Huete AR, Nobre AD, Artaxo P, Shimabukuro YE (2013) LBA-ECO CD-32 flux tower network data compilation. Brazilian Amazon: 1999–2006
Senay GB, Bohms S, Singh RK, Gowda PH, Velpuri NM, Alemu H, Verdin JP (2013) Operational evapotranspiration mapping using remote sensing and weather datasets: a new parameterization for the SSEB approach. J Am Water Resour Assoc 49(3):577–591
Shuttleworth WJ (1988) Evaporation from Amazonian rainforest. Proc R Soc B Biol Sci 233(1272):321–346
Simons G, Bastiaanssen WGM, Ngô LA, Hain CR, Anderson M, Senay G (2016) Integrating global satellite-derived data products as a pre-analysis for

hydrological modelling studies: a case study for the Red River Basin. Remote Sens 8(4)
Steduto P, Hsiao TC, Fereres E (2007) On the conservative behavior of biomass water productivity. Irrig Sci 25:189
Su Z (2002) The surface energy balance system (SEBS) for estimation of turbulent heat fluxes. Hydrol Earth Syst Sci 6(1):85–100
Teixeira AHC, Bastiaanssen WGM (2012) Five methods to interpret field measurements of energy fluxes over a micro-sprinkler-irrigated mango orchard. Irrig Sci 30(1):13–28
Tollefson J (2016) Deforestation spikes in Brazilian Amazon. Nature 540(7632): 182–182
Twine TE, Kustas WP, Normanc JM, Cookd DR, Houser PR, Meyers TP, Prueger JH, Starks PJ, Weselyd ML (2000) Correcting eddy-covariance flux underestimates over a grassland. Agric For Meteorol 103(3):279–300
van der Ent, Ruud J., A. Miriam J Coenders-Gerrits, Revekka Nikoli, and Hubert H G Savenije. 2012. The importance of proper hydrology in the forest cover-water yield debate. Global Change Biology, 18:806–820
Villar JCE, Ronchail J, Guyot JL, Cochonneau G, Naziano F, Lavado W, De Oliveira E, Vauchelh RP, Vauchel P (2009) Spatio-temporal rainfall variability in the Amazon basin countries (Brazil, Peru, Bolivia, Colombia, and Ecuador). Int J Climatol 29:1574–1594
von Randow C, Manzi AO, Kruijt B, Oliveira A, Zanchi FB, Silva RL, Hodnet MG, Gash JHC, Elbers JA (2004) Comparative measurements and seasonal variations in energy and carbon exchange over forest and pasture in South West Amazonia. Theor Appl Climatol 78(1–3):5–26
Wilson K (2002) Energy balance closure at FLUXNET sites. Agric For Meteorol 113(1–4):223–243
Wu B, Yan N, Xiong J, Bastiaanssen WGM, Zhu W, Stein A (2012) Validation of ETWatch using field measurements at diverse landscapes: a case study in Hai Basin of China. J Hydrol 436–437:67–80
Wang-Erlandsson L, Bastiaanssen WGM, Gao H, Jägermeyr J, Senay GB, van Dijk AIJM, Guerschman JP, Keys PW, Gordon LJ and Savenije HHG (2016) Global root zone storage capacity from satellite-based evaporation. Hydrol Earth Syst Sci, 20:1459–1481.